IMPACT OF ASSEMBLY-SPECIFIC CONDITIONS ON BWR BURNUP CREDIT

Brian J. Ade, William (B. J.) Marshall, and Stephen M. Bowman*
Oak Ridge National Laboratory
Oak Ridge, TN, USA
adebj@ornl.gov
marshallwj@ornl.gov
bowmansm@ornl.gov

ABSTRACT

Because boiling water reactors use control blades during operation, there can be significant changes to the local axial power shape, coolant density profile, and other parameters when the blades are inserted. Previous work examined the reactor operating parameters that impact cask reactivity. These previous studies identified limiting conditions for fuel cask reactivity or the direction of trends with cask reactivity (e.g., lower coolant densities result in higher cask reactivity). However, using limiting conditions for all parameters simultaneously is unrealistic. When the control blades are inserted deeply into the reactor—a limiting condition—the power is reduced and the void fraction decreases—a less limiting condition. This paper identifies the impacts of using assembly-specific conditions for control blade history, coolant density profile, burnup profile, and fuel temperature profile. Results indicate that cask reactivity is reduced when using assembly-specific operating conditions versus combining limiting conditions for the individual parameters of interest. The magnitude of reactivity reduction for using assembly-specific conditions varies based on each assembly and its operating conditions.

Key Words: **boiling water reactor, burnup credit, correlated conditions.**

1. INTRODUCTION

Applicants for certificates of compliance for spent nuclear fuel (SNF) transportation and dry storage systems perform analyses to demonstrate that these systems are adequately subcritical per the requirements of Title 10 of the Code of Federal Regulations (10 CFR) Parts 71 and 72 [1]. For SNF from pressurized water reactors (PWRs), these analyses may credit the reduction in assembly reactivity caused by depletion of fissile nuclides and buildup of neutron-absorbing nuclides during power operation. This credit for reactivity reduction during depletion is commonly referred to as *burnup credit* (BUC). US Nuclear Regulatory Commission (NRC) staff members review BUC analyses according to the Division of Spent Fuel Storage and Transportation Interim Staff Guidance (ISG) 8, Revision 3, "Burnup Credit in the Criticality Safety Analyses of PWR Spent Fuel in Transportation and Storage Casks" [2].

*This manuscript has been authored by UT-Battelle, LLC under Contract No. DE-AC05-00OR22725 with the U.S. Department of Energy. The United States Government retains and the publisher, by accepting the article for publication, acknowledges that the United States Government retains a non-exclusive, paid-up, irrevocable, world-wide license to publish or reproduce the published form of this manuscript, or allow others to do so, for United States Government purposes. The Department of Energy will provide public access to these results of federally sponsored research in accordance with the DOE Public Access Plan (http://energy.gov/downloads/doe-public-access-plan).

The technical basis for extended boiling water reactor (BWR) BUC (beyond peak reactivity) is being evaluated in an Oak Ridge National Laboratory (ORNL) research program under a contract with the NRC Office of Research. Research for peak reactivity BUC, which is defined as BUC at or before the burnup at which BWR fuel reactivity peaks due to depletion of burnable absorbers, is addressed in NUREG/CR-7194 [3] and Marshall's "Technical Basis for Peak Reactivity Burnup Credit for BWR Spent Nuclear Fuel in Storage and Transportation Systems" [4]. NUREG/CR-7158 [5] identifies and ranks parameters of importance to BWR BUC. NUREG/CR-7224 [6] summarizes impacts of the three highest-importance parameters: (1) axial coolant density distributions, (2) control blade usage, and (3) axial burnup profiles on extended BWR BUC [6–9]. The impacts of other lower importance operating parameters such as fuel temperature, operating history, specific power, and bypass water density were also previously researched [10].

Axial burnup profile, axial coolant density profile, and control blade usage, the three research objectives previously categorized as high priorities [5], were studied separately in NUREG/CR-7224 [6]. Each parameter was individually varied while the others were kept unchanged. This study investigated the effect of the correlation of these parameters. *Assembly-specific conditions*, also known as *correlated parameters*, are those conditions that are realistically experienced by an individual fuel assembly. For example, when the control blade is inserted, the assembly power, coolant density, and many other parameters all change accordingly. Modeling the assembly-specific conditions ensures that the operating parameters of interest are correlated. Previous studies [6] used uncorrelated data from different fuel assemblies that result in limiting cask reactivity estimates. The current work studies assembly-specific conditions to (1) confirm that using uncorrelated but limiting values for all operating conditions leads to conservative cask reactivity and (2) to further understand the magnitude of the impact that modeling assembly-specific conditions has on cask reactivity.

Using limiting values for the axial coolant density profile, burnup profile, control blade history, and other parameters will provide a conservative estimate of reactivity. However, simultaneous application of these limiting assumptions may be overly limiting. In reactor operation, it is unlikely that a fuel assembly would simultaneously experience a limiting control blade history (deeply inserted for long periods of time), a limiting coolant density profile (low moderation due to high power and increased boiling), and a limiting burnup profile (low burnup near the top of the fuel). This paper presents and assessment of the impacts of using true operating data correlated between the various conditions.

The studies documented herein were performed to determine the impact of using assembly-specific conditions for fuel depletion simulations on cask reactivity, rather than to provide a licensing basis for using an assembly-specific approach. While modeling assembly-specific conditions for every fuel assembly in a cask would be the most accurate approach, it may not be the most conservative or feasible approach. These studies were performed primarily to understand the level of conservatism (or non-conservatism) built into the simpler approach of using limiting conditions for all parameters of interest (coolant density profile, burnup profile, etc.).

2. METHODOLOGY

2.1. Codes, Methods, and Data

This study was performed using a series of codes and models to simulate fuel assembly irradiation and SNF reactivity in an SNF storage or transportation cask. The codes, associated data, and models used are summarized in this section. The assembly and cask configurations used in these studies are consistent with those used in NUREG/CR-7224 [6]. The computational procedure included the following main steps:

1. Perform depletion simulations to determine the isotopic composition of the irradiated fuel assembly at its discharge from the reactor.
2. Perform decay simulations of the discharged assembly's isotopic composition to determine the nuclides present at five years of cooling time after discharge from the reactor.
3. Perform criticality simulations for the GBC-68 cask to determine the effective multiplication constant (k_{eff}) using the isotopic composition of the SNF obtained in step 2.

These computational steps and the SCALE modules and codes used are illustrated in Figure 1 and are further described in this section. Version 6.2.1 of the SCALE code system [11] was used for all calculations in this work.

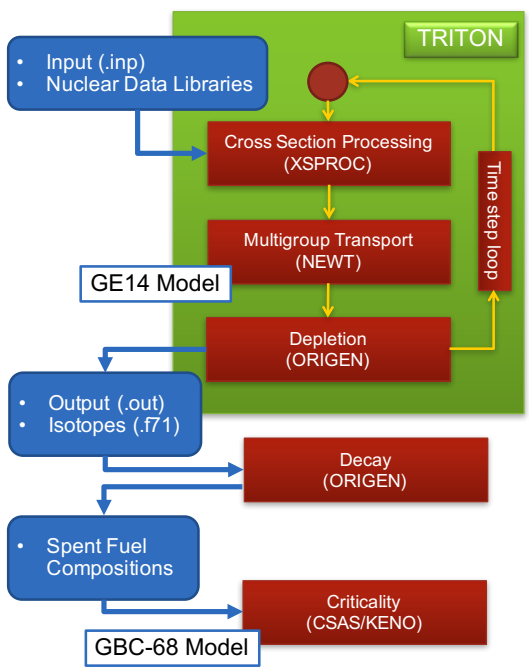

Figure 1. SCALE sequences and modules used for depletion and criticality calculations. TRITON is used to perform 2D depletion calculations for 25 axial levels (nodes) to model dominant (DOM or full) and vanished (VAN) lattices of the GE14 fuel assembly. The depleted fuel compositions are then decayed using ORIGEN and passed to KENO-V.a for criticality calculations in the GBC-68 fuel cask.

Through a joint NRC and ORNL project, the ORNL BWR BUC project gained access to proprietary

operating data for a single cycle of a BWR core. The data include inlet and outlet conditions and traveling in-core probe (TIP) data, as well as simulated core follow data for every fuel assembly in the reactor. The data were obtained from a recent cycle that contained multiple modern BWR fuel assembly designs. Each fuel assembly has been modeled with 25 different axial nodes, and the 690-day cycle was simulated using more than 240 time steps. The time step sizes vary slightly, but all steps are less than 5 effective-full-power days in length. State variables needed for the studies documented herein were extracted from the simulated data regardless of the specific assembly design. As a result, state variables from differing assembly designs have been applied to the GE14 assembly to isolate the impact of the variation of the operating conditions from the assembly design.

2.2. Models

GE14 is the only fuel assembly design used in these studies. This assembly has a 10 × 10 array of fuel pins and contains two large central water rods, each of which displaces four fuel rods. The GE14 fuel assembly can contain many axial levels with varying fuel enrichment and gadolinium loading. Due to the presence of part-length fuel rods which terminate at approximately half the total height of the fuel assembly, the GE14 fuel assembly contains two primary axial levels which are known as *zones*. These two axial zones are the DOM (dominant) and the VAN (vanished) lattices. A 2D slice through one of these axial zones is referred to as a *lattice*. The DOM lattice has fuel rods occupying every position in the fuel pin array. The vanished lattice is located axially above the part-length rods, so these rods are in effect removed or *vanished* from the lattice. TRITON representations of the DOM and VAN lattices are shown in Figure 2. All gadolinium-bearing rods contain the same absorber loading in both the DOM and VAN lattices. Axial enrichment zoning is not modeled for any calculations presented herein. Rather, all TRITON depletion calculations contain 4.5 wt% ^{235}U in all pins, with 7.0 wt% Gd_2O_3 in the gadolinia-bearing pins. The gadolinia-bearing pins have been modeled using seven radial rings, which provides a reasonable tradeoff between accuracy and CPU time required [12]. As indicated in Section 2.1, the core-follow data used contain 25 axial nodes, so 25 separate TRITON models are used to represent the axial variation of parameters in the assembly.

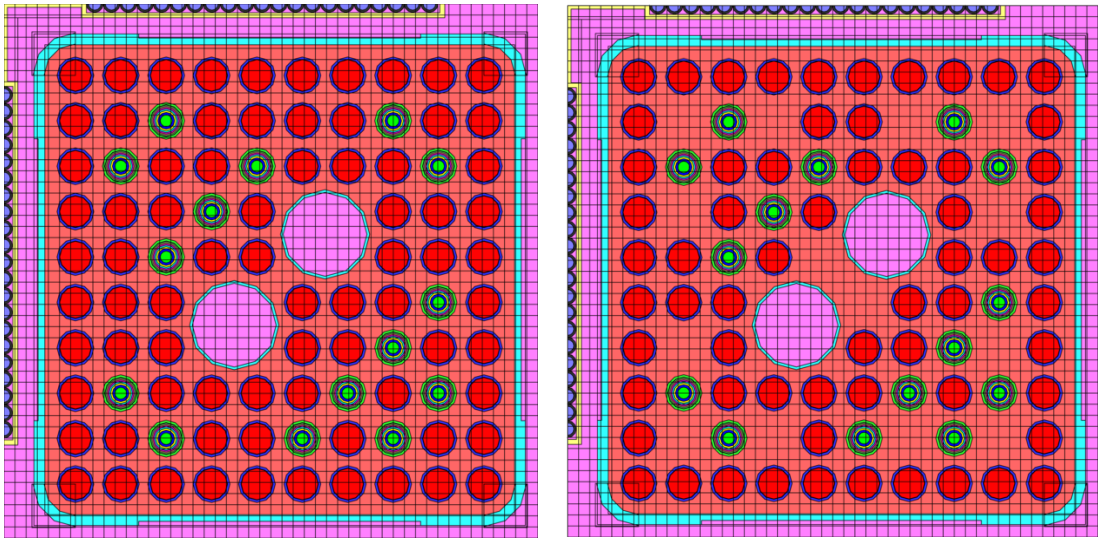

Figure 2. TRITON representations of the DOM (left) and VAN (right) lattices.

The GBC-68 computational benchmark model was developed in NUREG/CR-7157 [13] as a generic BUC cask for modeling BWR SNF. The KENO model of the fuel loaded in the cask explicitly represents each fuel rod, including its gap and cladding in the GE14 fuel assemblies. Part-length rods are truncated at the appropriate elevation so that both the DOM and VAN lattices are included explicitly in the KENO model. The fuel assembly channel model is simplified in KENO and is represented with constant thickness and squared corners. All fuel assemblies in the GBC-68 cask model are assumed to contain fuel with identical compositions and irradiation histories. KENO calculations performed with depleted fuel compositions generated by TRITON and ORIGEN assume a single average composition for fuel without gadolinium, as well as seven unique compositions for the rings modeling the gadolinium fuel pins in each axial node. All KENO models contain 25 axial nodes, each 6 inches in length (15.24 cm). Figure 3 shows a radial view of the GBC-68 half-cask model depicting the cask body, basket, and fuel assemblies.

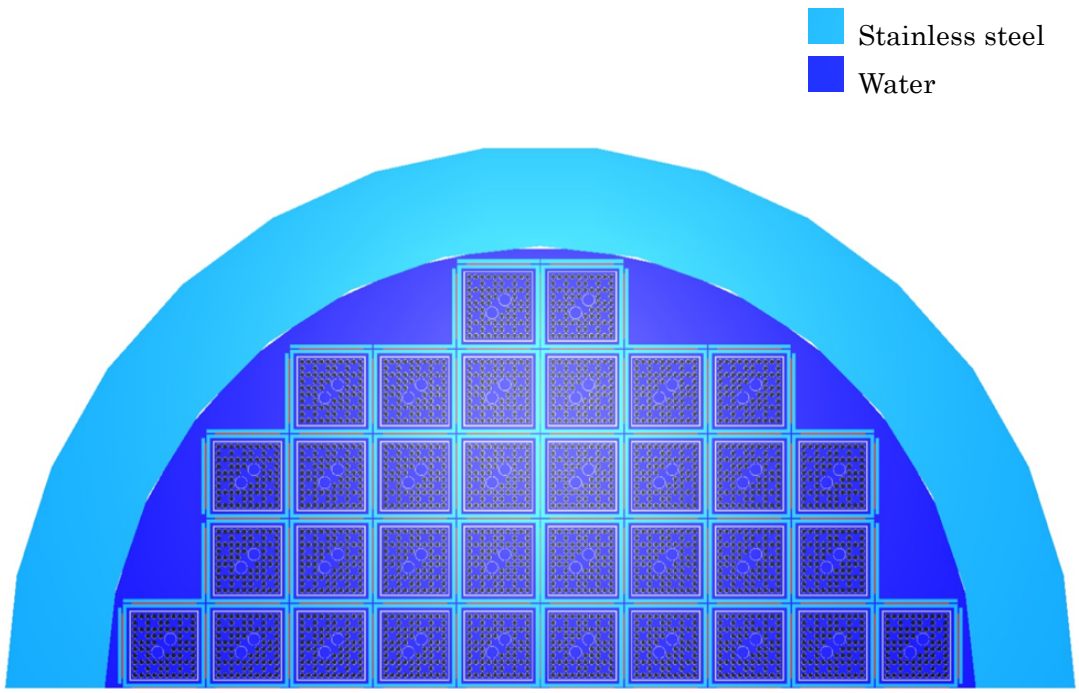

Figure 3. Radial view of the GBC-68 cask model in KENO in the VAN lattice.

Two sets of nuclides are used for fuel modeling in the KENO models: (1) major actinides only (AO), and (2) major and minor actinides and major fission products (AFP). The nuclides used in the AO and AFP nuclide sets are taken from NUREG/CR-7109 [14] and are the same as those typically used when performing PWR BUC calculations. The same isotope sets are used for BWR BUC studies because the same nuclides result from fission in both PWR and BWR types of light water reactors. The full set of nuclides for AO and AFP isotope sets is found in NUREG/CR-7224 [6].

2.2. Base Conditions

The study of the effect of assembly-specific conditions requires that base conditions for all parameters of interest first be established. The base conditions for the coolant density profile and axial burnup profile were chosen as the limiting conditions identified in NUREG/CR-7224 [6]. The base control blade history uses fully withdrawn control blades during the entire irradiation history because using fully inserted control blades for the entire irradiation period is overly limiting compared to realistic control blade histories [6]. The base fuel temperature profile is the highest time and spatially averaged temperature profile from the operating data.

2.3. Assembly-Specific Conditions

The assembly-specific (as-irradiated) conditions are obtained from the core-follow operating data. To study the impact of using assembly-specific conditions, a simulation is first performed using only the base conditions for all considered parameters. Then all subsequent calculations use this baseline case as a reference to assess the impact of including the assembly-specific parameters of interest. To test the impact of including as-irradiated conditions, the applicable conditions are substituted for base

conditions and the cask k_{eff} results are compared to the base conditions. For example, to assess the impact of assembly-specific control blade insertion, the base condition of control blades removed for the entire irradiation is replaced with an actual control blade history from a specific assembly. When the assembly-specific conditions are applied, the axial shape and time-dependence of these conditions are both simulated.

The three fuel assemblies chosen for analysis based on their control blade history are discussed in this section. Assembly 1 (A1) was chosen because it had the most limiting realistic control blade history, as detailed in NUREG/CR-7224 [6]. A1 contains two control blade insertions that were near full depth for a significant period of irradiation time. Assembly 2 (A2) was chosen because it had the most cumulative irradiation time during which the control blade was inserted (highest control blade history). Detailed control blade histories for A1 and A2 are provided at the end of this section. Assembly 3 (A3) was chosen as a control, as it contains no control blade insertion, but it has one of the most limiting burnup profiles identified in NUREG/CR-7224 [6]. Using A3 as the control will indicate whether the level of conservatism in the base conditions is due primarily to the burnup profile or the other operating conditions.

The cycle-averaged coolant void fraction profiles, axial burnup profiles, and fuel temperature profiles for the base condition and assembly-specific conditions for A1, A2, and A3 are plotted in Figure 4. The burnup profiles in Figure 4 have been normalized to an assembly-averaged burnup of 25 GWd/MTHM. The burnup profile plot in Figure 4 (middle) shows that although the base and A3 burnup profiles were taken from different fuel assemblies, they are very similar. The burnup profiles for A1 and A2 have much higher burnups at the tops of the fuel assemblies than those of A3. The coolant void fraction profile plot in Figure 4 (left) shows that the base void profile has a higher exit void fraction (lower coolant density) than the three assembly-specific profiles.

Five calculations are used for each selected assembly to assess the effects of the assembly-specific conditions. The base case uses base conditions for all parameters of interest. Case C uses the assembly-specific control blade history and base conditions for the coolant density, burnup profile, and fuel temperature. Case CV uses assembly-specific conditions for the control blade history and coolant density (void fraction, hence, *CV*) while base conditions are used for the burnup profile and fuel temperature. Likewise, case CVB uses assembly-specific conditions for the control blade history, coolant density, and burnup profile while the base fuel temperature is used. Finally, case CVBT uses assembly-specific conditions for all parameters being tested. The assembly-specific conditions are added one by one to enable estimation of the individual effects of each condition rather than just the total of all conditions.

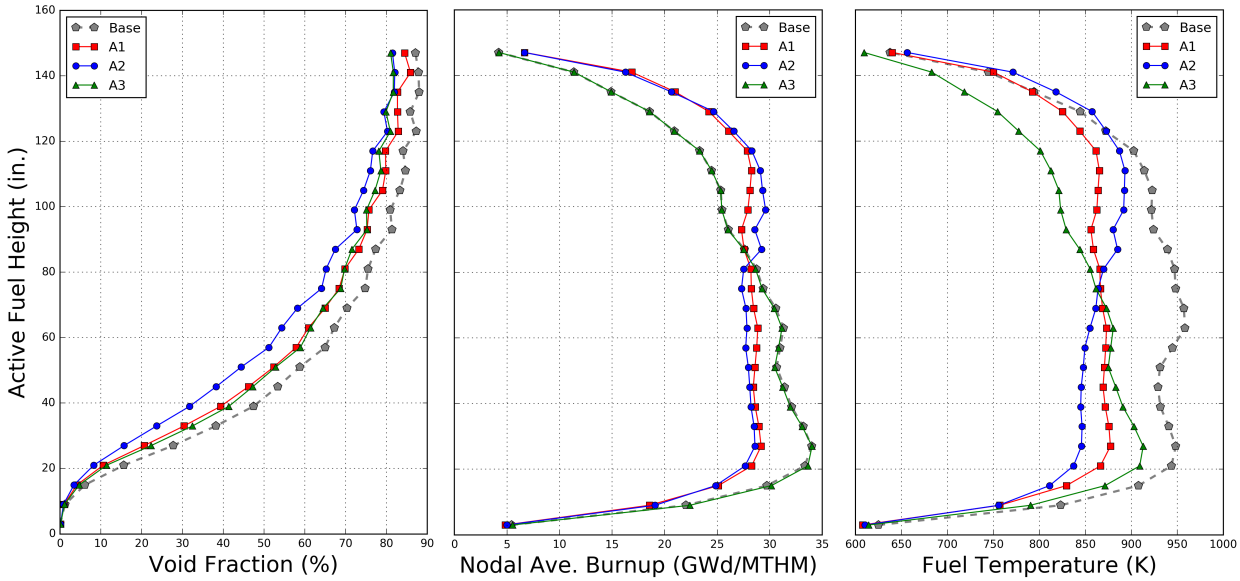

Figure 4. Base and assembly-specific cycle-average conditions for the coolant void fraction (left), axial burnup profile (middle), and fuel temperature axial profiles (right).

To model the control blade position as a function of irradiation time for a certain assembly, irradiation time is divided into intervals corresponding to constant control blade position. Figure 5 plots the control blade position as a function of time for A1 and A2. In Figure 5 (top), the cycle is divided into five time intervals in which the control blade is either fully withdrawn (gray) or inserted to some position (white). Circled numbers label the five different intervals.

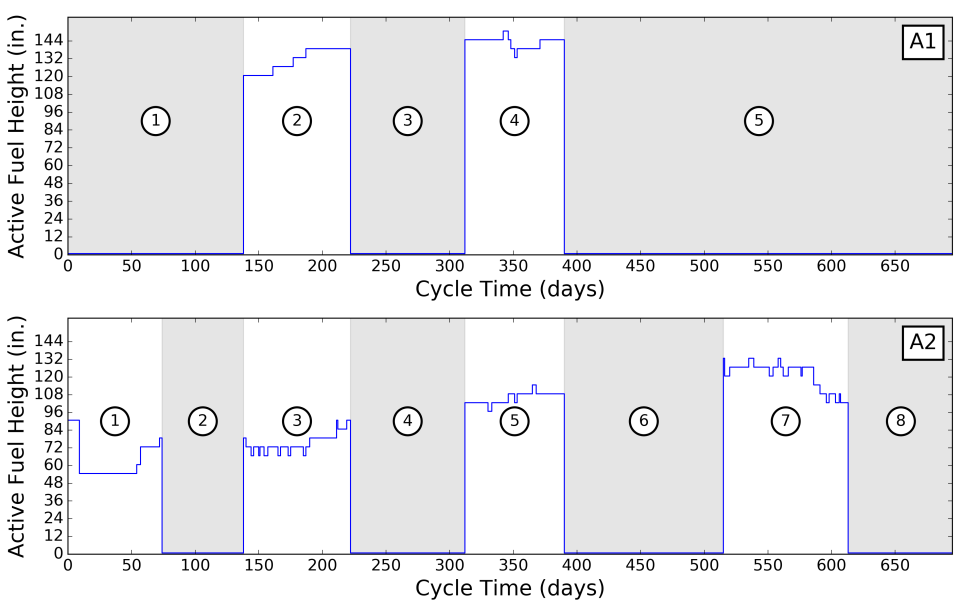

Figure 5. Control blade insertion depth as a function of time for assemblies A1 (top) and A2 (bottom).

In calculations that use assembly-specific conditions, both the axial- and time-dependence of the conditions are modeled. The actual operating data contain information on a finer timescale than the changes in control blade elevation. In the correlated parameter calculations, conditions of interest (nodal coolant density, nodal power, and nodal fuel temperature) are averaged over each time period for which the control blade position is constant. For example, interval 2 of A1 (Figure 5, top) is divided into four subintervals, the boundaries for which are defined by the interval over which the control blade position is constant. In each of the four subintervals in time interval 2, time-averaged coolant density, nodal power, and fuel temperature are used for each axial node. In interval 2, the axial shape of the assembly-specific conditions is updated four times. The assembly-specific conditions are averaged over any interval during which the control blade position is constant. The power for all cases is normalized such that the assembly-average burnup is 25 or 50 GWd/MTHM, depending on the case being tested.

3. RESULTS

The effect of assembly-specific conditions on cask reactivity are plotted in Figures 6 and 7 for AO and AFP isotope sets at assembly-average discharge burnups of 25 and 50 GWd/MTHM, respectively. The dashed lines in these figures indicate the base case reactivity (Δk_{eff} is zero). As shown in Figure 4, the base cases assumed limiting conditions and control blades completely withdrawn. Any data above this dashed line represent an increase in cask reactivity above the base conditions, and any data below the dashed line represent a decrease in cask reactivity relative to base conditions.

For A1 and A2, use of the assembly-specific control blade history (C cases) results in a relatively small impact on cask reactivity of less than 1% Δk_{eff} for both AO and AFP isotope sets. Although these studies are slightly different, this result aligns well with the results in NUREG/CR-7224 [4], indicating an impact of less than 1% on cask reactivity for realistic control blade usage.

Addition of the assembly-specific coolant density profile to the assembly-specific control blade history results in a reduction in reactivity for all cases, although the magnitude of the reduction depends largely on the assembly-specific coolant density profile itself. The reduction in reactivity when comparing C to CV is larger (~500 pcm, or 0.5% Δk_{eff}) for A2 than for the other two assemblies. This is primarily caused by a less limiting coolant density profile (Figure 4) for A2 compared to A1 and A3. Overall, using the assembly-specific control blade and coolant density data results in small impacts to cask reactivity.

As shown in Figure 6, the largest impact to cask reactivity for the assemblies that contain control blade insertion is clearly the addition of the assembly-specific burnup profile. For the rodded assemblies (A1 and A2), the burnup profile is worth 2–3% Δk_{eff} at 25 GWd/MTHM when comparing CV to CVB. Realistic control blade insertion alone does not have a significant impact on cask reactivity, but the presence of the control blade during irradiation tends to result in a less-limiting burnup profile. Because control blades in BWRs are inserted from the bottom of the assembly, the power and therefore the burnup profile tend to be more top-peaked during periods of control blade insertion. This leads to a reduction in fissile ^{235}U in the upper portion of the fuel assembly, resulting in a large change in reactivity compared to the limiting burnup profile. For all cases, the impact of including fuel temperature is very small compared to inclusion of the other three operating conditions.

Results for A3 are differ significantly from the results for A1 and A2. This is largely due to the difference in the operating history for A3 compared to operating histories for A1 and A2. A1 and A2 were chosen specifically because their operating histories include significant control blade insertion which leads to changes to other assembly-specific conditions. A3 was chosen because it has no control blade insertion and has one of the more limiting burnup profiles. Because A3 has no control blade insertion, there is little impact to using the assembly-specific conditions for that fuel assembly. However, cask reactivity is slightly lowered by using the assembly-specific conditions for A3, which is primarily due to its less limiting coolant density profile. The magnitude of the reduction in cask reactivity for A3 is much smaller than that obtained for A1 or A2.

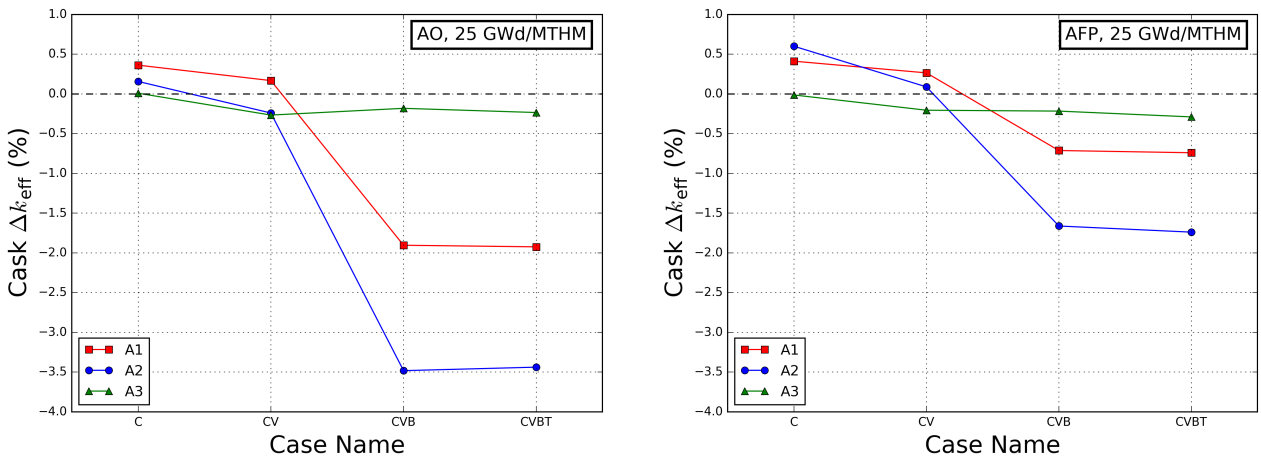

Figure 6. Cask Δk_{eff} values for the AO (left) and AFP (right) isotope sets at an assembly average discharge burnup of 25 GWd/MTHM.

The effect of assembly-specific conditions on cask reactivity can be found in Figure 7 for the AO and AFP isotope sets at an assembly average discharge burnup of 50 GWd/MTHM. The C and CV cases have Δk_{eff} values similar to those of the 25 GWd/MTHM cases, but the impact of the burnup profile is much larger at 50 GWd/MTHM than at 25 GWd/MTHM. The larger impact of the burnup profile compared to the other parameters is due to the more top-peaked fission density axial profiles for the 50 GWd/MTHM cases, as discussed below. In these studies, full-length fuel without natural uranium blankets were modeled; as such, the impact of the burnup profile and other parameters would change depending on the assumptions used to model the fuel assembly.

The shape of the curves in Figure 7 are similar to those in Figure 6, but the impact of the assembly-specific conditions is significantly greater at assembly average burnups of 50 GWd/MTHM than at 25 GWd/MTHM. Specifically, the impact of adding the assembly-specific burnup profile is more significant at 50 than at 25 GWd/MTHM. This is caused by the shape of the axial fission distribution at 25 GWd/MTHM, which is less top-peaked than at 50 GWd/MTHM. Plots of the axial fission distributions for the CVBT cases for the AO and AFP isotope sets at 25 and 50 GWd/MTHM are shown in Figure 8. As discussed in this and previous reports [6], the fission density distribution in the top axial portion of the fuel assembly plays a major role in cask reactivity. The more top-peaked the distribution is, the higher the impact of the burnup profile on cask reactivity [6]. The cases considered

here have a less top-peaked fission distribution at 25 GWd/MTHM compared to that for 50 GWd/MTHM, so the importance of the assembly-specific burnup profile is smaller at 25 GWd/MTHM than at 50 GWd/MTHM.

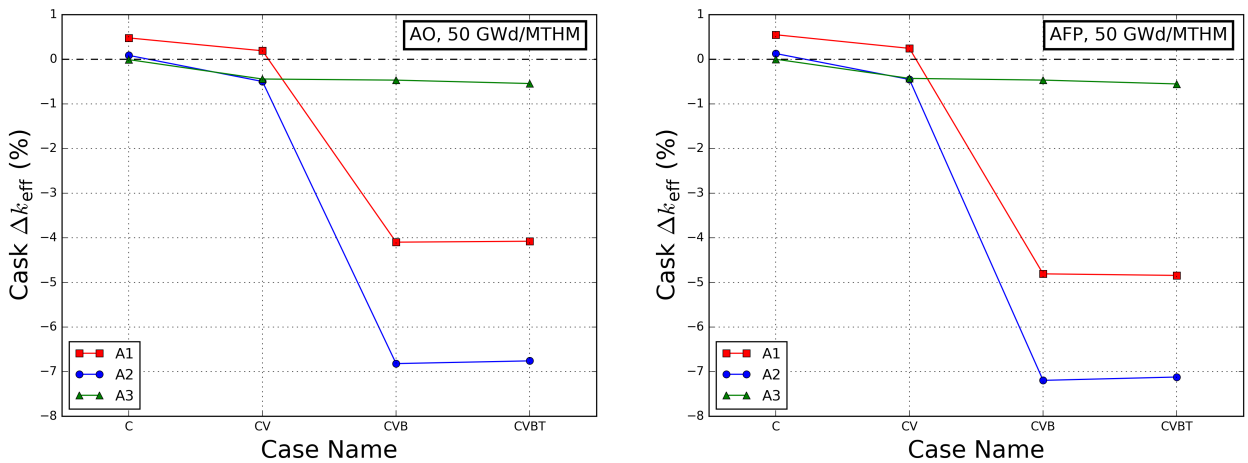

Figure 7. Cask Δk_{eff} values for the AO (left) and AFP (right) isotope sets at an assembly average discharge burnup of 50 GWd/MTHM.

As shown in Figure 4, the base burnup profile has much lower burnup values at the top of the fuel assembly compared to those in the A1 assembly profile. Correlating that with the more top-peaked fission distribution at 50 GWd/MTHM as shown in Figure 8 indicates that the impact of the burnup profile for higher burnups is primarily due to the large difference in the burnup profiles at the top of the fuel assembly.

The less top-peaked fission density distribution at 25 GWd/MTHM is a result of the combined impact of the increased residual ^{235}U in the middle axial regions of the fuel assembly, the lower concentration of ^{239}Pu at the top of the assembly, and the higher concentration of residual gadolinium in the top of the fuel assembly. Figure 9 shows the ^{235}U, ^{239}Pu, and ^{155}Gd concentration plotted as a function of axial position for assembly A1.

The distribution of the ^{235}U concentration as a function of axial position follows an inverse shape of the burnup profile: it has higher concentrations for lower burnup regions and lower concentrations for higher burnup regions. At both 25 and 50 GWd/MTHM, the ^{235}U concentration is higher at the axial ends of the fuel assembly than in the middle portions of the fuel assembly. Comparing the ^{239}Pu concentration as a function of axial position for the two selected burnups (Figure 9, middle) reveals that the 50 GWd/MTHM burnup results in higher plutonium concentrations in the top axial portion of the assembly. For the gadolinium burnable absorber, the 25 GWd/MTHM case results in higher ^{155}Gd concentrations in the top and bottom of the assembly due to the lower burnup at the ends of the fuel assembly.

The fission distribution for the AO isotope set (Figure 8, left), which does not contain gadolinium, shows that the 50 GWd/MTHM case is more top-peaked than the 25 GWd/MTHM case. However, it

is clear that the gadolinium has an impact at 25 GWd/MTHM, as seen by comparing the fission distributions for the AO and AFP isotope sets in Figure 8. The AFP fission distribution is clearly less top-peaked than the AO fission distribution at 25 GWd/MTHM.

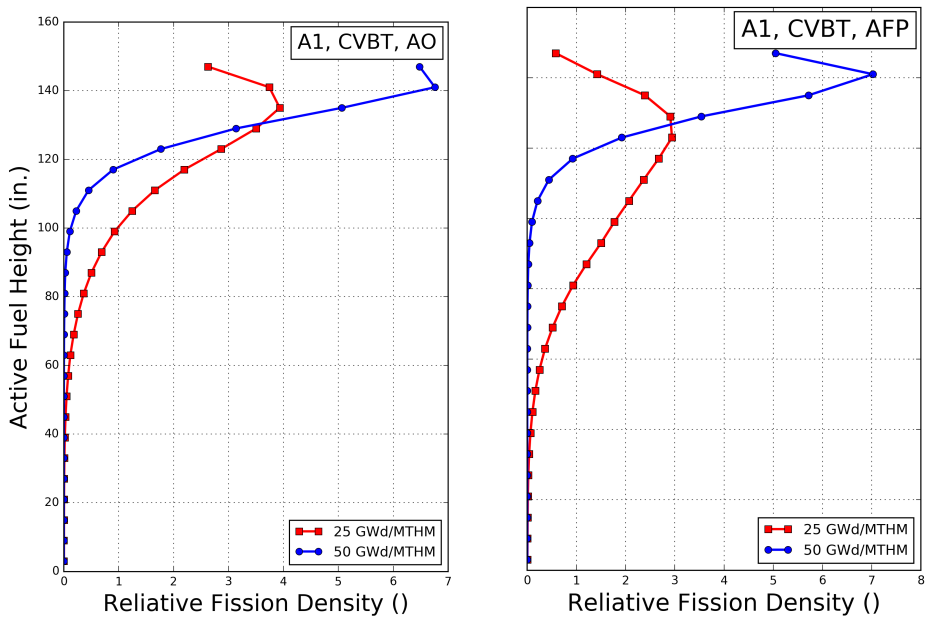

Figure 8. Axial fission distribution for assembly A1 CVBT case at assembly average discharge burnup values of 25 and 50 GWd/MTHM for the AO and AFP isotope sets.

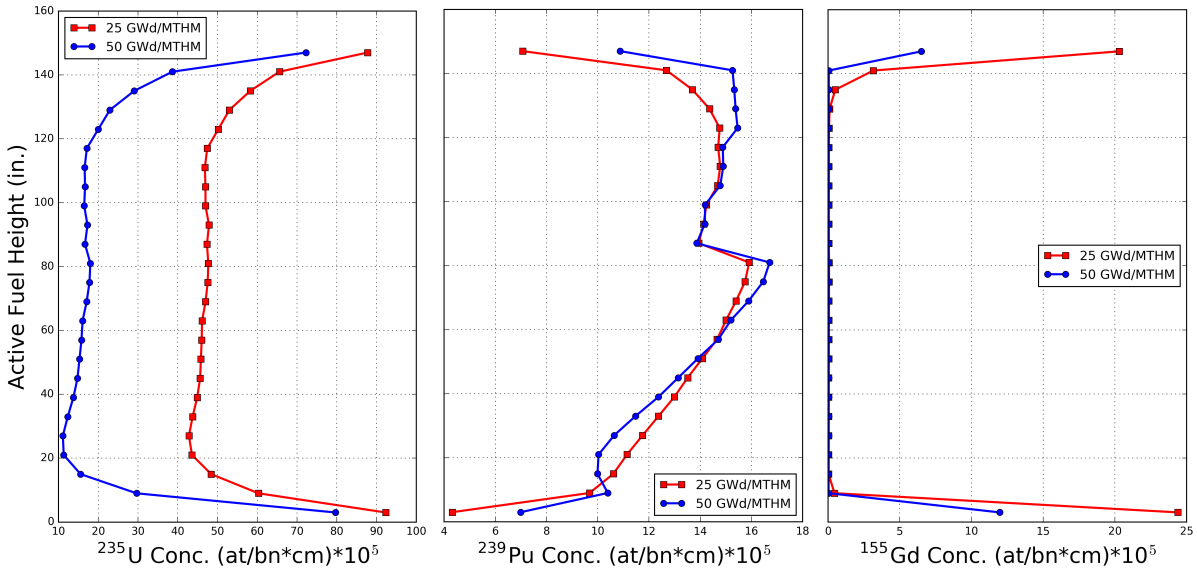

Figure 9. ^{235}U (left), ^{239}Pu (middle), and ^{155}Gd (right) concentration for A1 CVBT case at 25 and 50 GWd/MTHM.

4. CONCLUSIONS

The impact of the correlation of major operating conditions, coolant density profile (void profile), control blade history, and axial burnup profile varies with each fuel assembly. Using limiting conditions for the coolant density profile, control blade history, and axial burnup profile will result in conservative cask reactivities compared to the use of assembly-specific conditions. The impacts of assembly-specific conditions were evaluated for 25 and 50 GWd/MTHM assembly average discharge burnups. The assembly-specific conditions were studied for three different assemblies. The results obtained using these three assemblies are unlikely to bound all possibilities for all reactors. Additional research is needed using multiple cycles of data from additional reactors to fully assess the impacts of assembly-specific conditions. The major conclusions of this study are summarized below.

- Cask reactivity is reduced by using assembly-specific conditions compared to limiting conditions for the major operating conditions. The magnitude of this reactivity reduction ranges from ~0.50% Δk_{eff} to more than 7% Δk_{eff}, depending on the assembly and assembly-specific conditions included.
- Using the assembly-specific burnup profile has the most significant impact on cask reactivity, which is consistent with previous findings. The impact varies significantly according to the assembly selected.
- The impact of assembly-specific conditions on cask reactivity is greatest for assemblies with significant control blade insertion. Use of the control blade during operation changes the axial shape of the coolant density and burnup profile. Insertion of the control blade leads to less limiting coolant density and burnup axial profiles.
- The impacts of assembly-specific conditions on cask reactivity are greater for high discharge burnups than for low discharge burnups.

The results from previous studies [6,7] and the studies documented in this paper indicate that the axial burnup profile has the greatest impact on cask reactivity of any studied parameter. The significant impact to cask reactivity is due to the top-peaked axial fission distribution in BWR spent fuel casks that is caused by the low burnup in the axial top portion of BWR fuel assemblies combined with the ^{239}Pu generated by the harder neutron flux spectrum in the top of the reactor core. The next largest impact on cask reactivity is the axial coolant density distribution. Limiting coolant density distributions have low coolant density at the top of the fuel assembly, leading to increased plutonium production. The impact of realistic control blade histories is relatively minor because few assemblies experience near full-depth control blade insertion for significant periods or irradiation. The impact of modeling assembly-specific conditions that are correlated can provide cask reactivity reductions, but the magnitude of the reduction varies significantly with each fuel assembly.

ACKNOWLEDGMENTS

Funding for this work was provided by the US Nuclear Regulatory Commission (NRC). The authors would like to thank the NRC staff for their helpful comments and their support of this work. Special thanks are extended to Justin Clarity and Ugur Mertyurek from Oak Ridge National Laboratory for reviewing this paper and providing valuable suggestions, and Rose B. Raney for editing the document.

REFERENCES

[1] US Code of Federal Regulations Title 10, "Energy," US Nuclear Regulatory Commission, Washington, DC (2017).

[2] Division of Spent Fuel Storage and Transportation, Interim Staff Guidance – 8, Revision 3, "Burnup Credit in the Criticality Safety Analyses of PWR Spent Fuel in Transportation and Storage Casks," US Nuclear Regulatory Commission (September 26, 2012).

[3] W. J. Marshall, B. J. Ade, S. M. Bowman, I. C. Gauld, G. Ilas, U. Mertyurek, and G. Radulescu, *Technical Basis for Peak Reactivity Burnup Credit for BWR Spent Nuclear Fuel in Storage and Transportation Systems*, NUREG/CR-7194 (ORNL/TM-2014/240), prepared for the US Nuclear Regulatory Commission by Oak Ridge National Laboratory, Oak Ridge, Tennessee (April 2015).

[4] W. J. Marshall, B. J. Ade, S. M. Bowman, I. C. Gauld, G. Ilas, U. Mertyurek, and G. Radulescu, "Technical Basis for Peak Reactivity Burnup Credit for BWR Spent Nuclear Fuel in Storage and Transportation Systems," *Proc. International Conference on Nuclear Criticality Safety*, Charlotte (September 2015).

[5] D. E. Mueller, S. M. Bowman, W. J. Marshall, and J. M. Scaglione, *Review and Prioritization of Technical Issues Related to Burnup Credit for BWR Fuel*, NUREG/CR 7158 (ORNL/TM 2012/261), prepared for the US Nuclear Regulatory Commission by Oak Ridge National Laboratory, Oak Ridge, Tennessee (February 2013).

[6] W. J. Marshall, B. J. Ade, S. M. Bowman, and J. S. Martinez, *Axial Moderator Density Distributions, Control Blade Usage, and Axial Burnup Distributions for Extended BWR Burnup Credit*, NUREG/CR-7224 (ORNL/TM-2015/544), prepared for the US Nuclear Regulatory Commission by Oak Ridge National Laboratory, Oak Ridge, Tennessee (August 2016).

[7] B. J. Ade, W. J. Marshall, S. M. Bowman, I. C. Gauld, G. Ilas, and J. S. Martinez, "Coolant Density and Control Blade History Effects in Extended BWR Burnup Credit," *Proc. International Conference on Nuclear Criticality Safety*, Charlotte (September 2015).

[8] B. J. Ade, W. J. Marshall, and J. S. Martinez, "Effect of Control Blade History, and Axial Coolant Density and Burnup Profiles on BWR Burnup Credit," *Proc. of PHYSOR 2016*, Sun Valley, ID (May, 2016).

[9] W. J. Marshall, B. J. Ade, S. M. Bowman, "Study of Axial Burnup Profile Effects on BWR Burnup Credit," *Proc. of PATRAM 2016*, Kobe, Japan (September 2016).

[10] G. Ilas, B. R. Betzler, B. J. Ade, "Impact of Reactor Operating Parameters on Cask Reactivity in BWR Burnup Credit," *Proc. of PATRAM 2016*, Kobe, Japan (September 2016).

[11] *SCALE: A Comprehensive Modeling and Simulation Suite for Nuclear Safety Analysis and Design*, ORNL/TM-2005/39, Version 6.2.1, Oak Ridge National Laboratory, Oak Ridge, Tenn. (August 2016). Available from Radiation Safety Information Computational Center at Oak Ridge National Laboratory as CCC-834.

[12] B. J. Ade, *SCALE/TRITON Primer: A Primer for Light Water Reactor Lattice Physics Calculations*, NUREG-7041 (ORNL/TM-2011/21), prepared for the US Nuclear Regulatory Commission by Oak Ridge National Laboratory, Oak Ridge, Tennessee (November 2012).

[13] D. E. Mueller, J. M. Scaglione, J. C. Wagner, and S. M. Bowman, *Computational Benchmark for Estimated Reactivity Margin from Fission Products and Minor Actinides in BWR Burnup Credit*, NUREG/CR-7157 (ORNL/TM-2012/96), prepared for the US Nuclear Regulatory

Commission by Oak Ridge National Laboratory, Oak Ridge, Tennessee (February 2013).

[14] J. M. Scaglione, D. E. Mueller, J. C. Wagner, and W. J. Marshall, *An Approach for Validating Actinide and Fission Product Burnup Credit Criticality Safety Analyses – Criticality (k_{eff}) Predictions*, NUREG/CR-7109 (ORNL/TM-2011/514), prepared for the US Nuclear Regulatory Commission by Oak Ridge National Laboratory, Oak Ridge, Tenn. (April 2012).